A. Arrizabalaga et al., "Impact of silicon carbide devices in 2 MW DFIG based wind energy system," 2020 22nd European Conference on Power Electronics and Applications (EPE'20 ECCE Europe), Lyon, France, 2020, pp. P.1-P.10.

DOI: https://doi.org/10.23919/EPE20ECCEEurope43536.2020.9215729

Impact of silicon carbide devices in 2 MW DFIG based wind energy system

Antxon Arrizabalaga[1], Aitor Idarreta[1], Mikel Mazuela[1], Iosu Aizpuru[1], Unai Iraola[1]
José Luis Rodriguez[2], Daniel Labiano[2], Ibrahim Alişar[3]

[1] MONDRAGON UNIBERTSITATEA
Fundazioa eraikuntza; Jauregi Bailara, z.g, 20120 Hernani, Spain
Tel.: +34 / +(34) – 943794700.
E-Mail: aarrizabalaga@mondragon.edu
URL: https://www.mondragon.edu/

[2] SGRE INNOVATION & TECHNOLOGY S.L.
Avda Ciudad de la Innovación 2 Sarriguren, Spain
Tel.: +34 / +(34) – 948771000.
E-Mail: jose.l.rodriguez@siemensgamesa.com
URL: https://www.siemensgamesa.com/en-int

[3] SIEMENS GAMESA RENEWABLE ENERJI A.S.
Adalet Mah. Sehit Polis Fethi Sekin Cad. No:4/64 Bayrakli Izmir, Turkey
Tel.: +90 / +(90) – 5056757220
E-Mail: ibrahim.alisar@siemensgamesa.com
URL: https://www.siemensgamesa.com/en-int

Keywords

«Wind energy», «Modeling», «DFIG», «SiC», «Volume reduction».

Abstract

Renewable energies are going through a major increment, mainly wind and photovoltaic energies, being market competitiveness the main driver for their massive penetration. As power converters are used to interface renewable energy systems with the utility grid, their optimization is crucial. For their superior conduction and switching capabilities, silicon carbide (SiC) semiconductors are considered for their use in the optimization of power electronics in doubly fed induction generator (DFIG) based wind energy systems (WES). Potential efficiency gain and volume reduction due to the use of SiC semiconductors are studied by simulation, explaining the models in detail. Commercial products are evaluated to calculate cooling systems (CS) and output filters volumes. The performance and volume of SiC converter is analyzed and compared to its Si counterpart, at different wind speeds and switching frequencies. A design for maximum efficiency and minimum CS volume, and another for minimum output filters volume without efficiency penalty are achieved. A switching frequency optimization is performed to obtain the minimum combined volume between the CS and output filter, still improving the Si converters efficiency at nominal wind speed conditions. The conclusion is that SiC semiconductors can improve the power converters efficiency and overall size in DFIG WES.

Introduction

The use of conventional energy generation sources has increased the concern of reaching the irreversible climate change point in the planet (this last decade has been the hottest one since data is collected [1]). For this reason, a radical energy revolution is needed in our society and ruling organizations are working in this direction. The United Nations 2030 Agenda will try to "Ensure access to affordable, reliable, sustainable and modern energy for all" [2]. In addition, one of the Horizon Europe research initiative missions is "Adaptation to climate change including societal transformation" [3].

Renewable energies have gone through a major increment in their use. By the end of 2018, the renewable energies represented the 26.2 % of the world energy mix, having experienced a growth of 33 % in the last year [4]. In addition, hydro, solar, wind, tidal and biomass have been receiving increasing attention

from engineers, developers and scientific community in general since the 2000s [5], [6], being Photovoltaic (PV) and Wind Energy Systems (WES) the main actors in the current scenario [4].

Market competiveness is the main driver for renewable energies high penetration into the energy mix [7]. To improve this market competiveness, the system cost must be optimized in wind and solar energy generation systems. In both energy generation systems power converters are used to interface with the distribution grid [8]–[10], however, the use of power electronics lead to high losses, reducing the efficiency and final available energy [11][12]. Silicon carbide (SiC) power semiconductors are identified as a potential technology to overcome the before mentioned drawback in WES, in small scale turbines [13]–[15] and MW power range [9], [16]–[18]. In addition, the use of SiC devices lower cooling systems (CS) and output filters volume and weight, making a direct impact on the system cost and decreasing the WES levelized cost of energy (LCOE) [13], [17], [19], [20].

As shown in the previous paragraph, there is wide literature work done analyzing the impact SiC devices can have in fully rated wind power converters; however, main wind turbine manufacturers (Vestas, Siemens-Gamesa, Acciona, General Electric, Mitsubishi, Alstom, Repower, e.g.), offer partial power converter systems, based on doubly fed induction generators (DFIG) in the range of 2 MW. As the converter processes only around 30 % of the power [21], this paper addresses the impact SiC devices can offer in DFIG based WESs.

DFIG based wind energy system modeling

Based on a 2 MW DFIG wind turbine example in [21], the system shown in Fig. 1, is modeled. It is composed of a 2 MW wind turbine, a DFIG with 2 pole pairs and a nominal stator voltage of 690 V, a back-to-back converter connected to the rotor with its CS and a utility line filter, Fig. 2. The inputs of the system are the wind speed, the switching frequency of the converter, the ambient and junction temperature. The outputs are the volumes of the CS and the filter, as well as the efficiencies of the converter and the generator. The models are connected by sharing variables. Three different semiconductor technologies are analyzed, state of the art Si IGBTs, “hybrid” devices composed by a Si IGBT and a SiC diode, and full SiC MOSFETs. Every component’s modeling is addressed in the following sections.

Wind turbine model

The wind turbine model is mainly based on the aerodynamic behavior of a 2 MW wind turbine available in one of the examples in [21]. Look-up tables are used to predict the wind turbine performance in every operation point. The tip speed ratio is estimated depending on the wind speed, and using the data provided in the manufacturers brochures, the mechanical power in the generators high speed shaft is calculated. The working wind speed range of the selected wind turbine goes form 3 to 25 m/s.

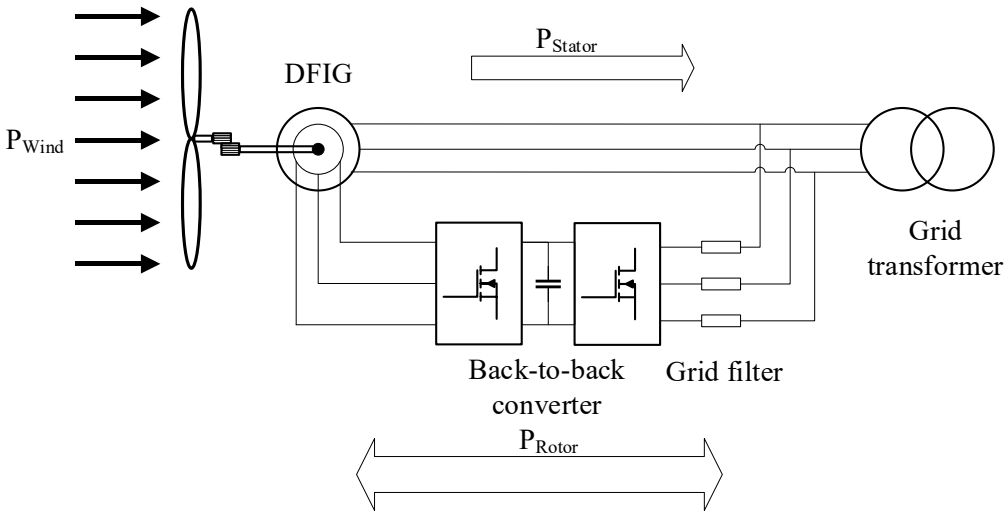

Fig. 1: DFIG based WES.

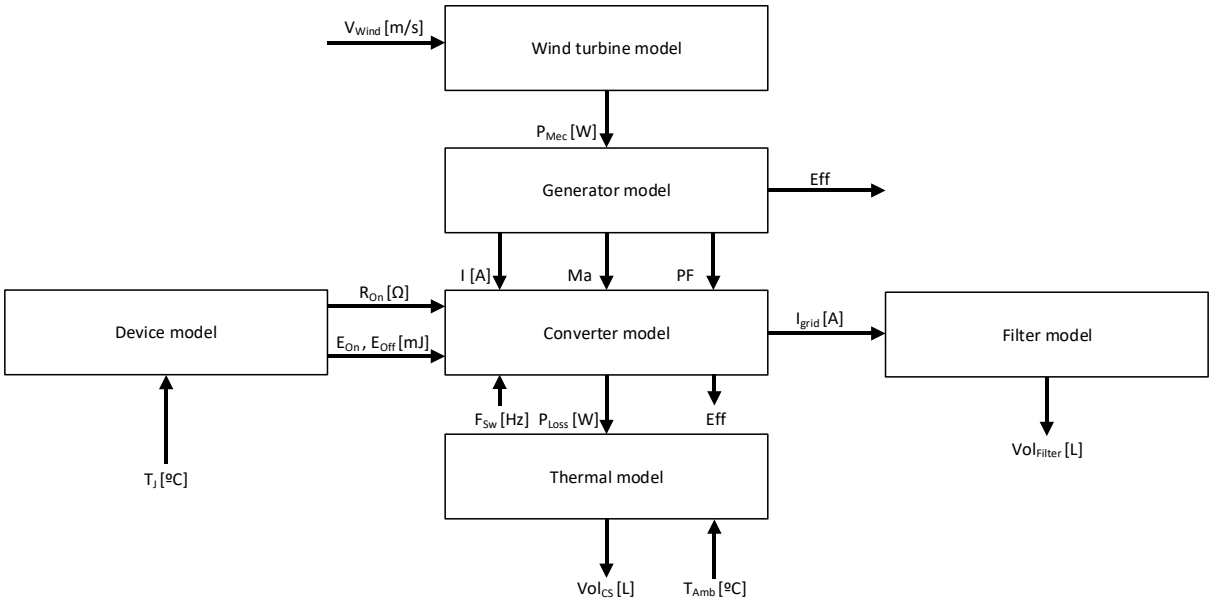

Fig. 2: WES model diagram.

Generator model

The generator model is based on analytical equations derived from the DFIG electrical model [21]. The input of the model is the mechanical power delivered by the wind turbine to the generators shaft. Depending on the mechanical speed, the rotor consumes power from the grid, (sub synchronous operation) or delivers power to the grid (hyper synchronous operation). In synchronous speed, the power in the rotor is ideally zero [21], being also the power managed by the power converter zero. Close to this operation point, the generator delivers very low currents to the converter Fig. 3.

Device model

The device model provides the on and off energies required to switch each semiconductor, as well as the conduction model. These data are obtained from the manufacturers brochures for Si, hybrid and full SiC technologies. Fig. 4 shows the performance comparison between the selected technologies. As it can be seen in Fig. 4 (a), the SiC MOSFET performs nearly as a resistive component in conduction, while Hybrid and the Si IGBTs have a direct voltage drop in conduction. This characteristic makes SiC MOSFETs more efficient in conduction at low currents, which occur close to synchronous speed according to Fig. 3.

Fig. 4 (b) analyzes the switching performances. Due to the unipolar nature of the MOSFET structure, the tail currents that are present when switching bipolar devices are eliminated, achieving much lower switching energies. This allows to increase switching frequency without penalizing efficiency drastically with SiC MOSFETs, as it would occur with Si IGBTs and Hybrid devices. Table I shows the semiconductors used in this paper.

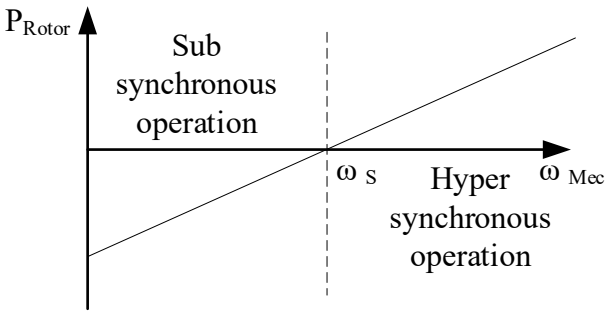

Fig. 3: Power managed by the rotor in a DFIG depending on the mechanical angular speed of the shaft.

Table I: Devices used in the paper

Technology	Voltage rating [V]	Current rating [A]	Generator side configuration	Grid side configuration	Part number
Si IGBT	1700	600	3 modules in parallel	2 modules in parallel	SKiiP 3614
Hybrid	1700	400	4 modules in parallel	2 modules in parallel	2MSI400VA E-170-53
SiC MOSFET	1700	225	6 modules in parallel	3 modules in parallel	CAS300M17 BM2

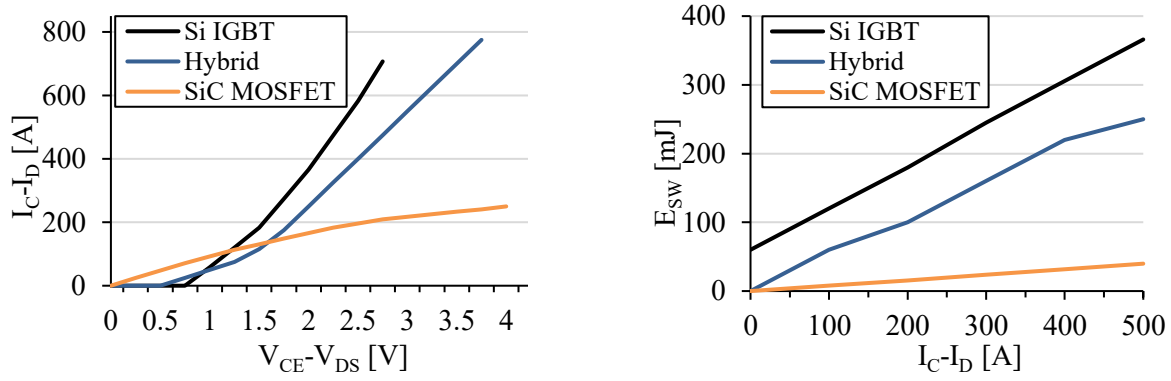

(a) (b)

Fig. 4: Selected Si IGBT, Hybrid and SiC MOSFETs performance comparison, (a) in conduction, (b) switching.

Converter model

The converter model uses analytical equations to describe the converters performance in every operation point. As it can be seen in Table I, the currents in the generator side are higher, needing more modules in parallel to operate in safe conditions. The converter is a 2L-Voltage Source Converter (2L-VSC) driven by a PWM modulation, with a defined and fixed switching frequency. The converter model calculates conduction and switching losses. In this point, it is important to remark the power processed by the converter is only the power managed by the rotor, and not all the power generated by the wind turbine, Fig. 1. Next, the equation list used to obtain the power losses in the converter is shown:

The generic conduction loss expression for every semiconductor is (1) [22].

$$P_{Cond} = V_{th} \cdot I_{AV} + R_{ON} \cdot I_{RMS}^2 \tag{1}$$

Being (2) the resultant equation for a MOSFET, (3) for an IGBT and (4) in the case of a diode and for a 2L-VSC. ma is the modulation index, (5). The parameters for each semiconductor are introduced in the corresponding equations, and conduction power losses calculated. The V_{th} factor present in the equations referring to IGBTs and diodes is the representation of the direct voltage drop in conduction, analyzed in Fig. 4 (a).

$$P_{\text{Cond\_MOSFET}} = \frac{1}{2} \cdot \left(R_{\text{ON}} \cdot \frac{I_{\text{max}}^2}{4} \right) + ma \cdot \cos(\varphi) \cdot \left(\frac{R_{\text{ON}} \cdot I_{\text{max}}^2}{3 \cdot \pi} \right) \tag{2}$$

$$P_{\text{Cond\_IGBT}} = \frac{1}{2} \cdot \left(V_{\text{th}} \cdot \frac{I_{\text{max}}}{\pi} + R_{\text{ON}} \cdot \frac{I_{\text{max}}^2}{4} \right) + ma \cdot \cos(\varphi) \cdot \left(V_{\text{th}} \cdot \frac{I_{\text{max}}}{8} + \frac{R_{\text{ON}} \cdot I_{\text{max}}^2}{3 \cdot \pi} \right) \tag{3}$$

$$P_{\text{Cond\_DIODE}} = \frac{1}{2} \cdot \left(V_{\text{th}} \cdot \frac{I_{\text{max}}}{\pi} + R_{\text{ON}} \cdot \frac{I_{\text{max}}^2}{4} \right) - ma \cdot \cos(\varphi) \cdot \left(V_{\text{th}} \cdot \frac{I_{\text{max}}}{8} + \frac{R_{\text{ON}} \cdot I_{\text{max}}^2}{3 \cdot \pi} \right) \tag{4}$$

$$ma = \sqrt{2} \cdot \frac{V_{\text{ll}}}{V_{\text{dc}}} \tag{5}$$

Switching losses are calculated using (6) in a 2L-VSC. The parameters a, b and c refer to the coefficients of the second order polynomial that approaches the switching energy losses curve provided in the datasheet, shown in Fig. 4 (b), as done in [16].

$$P_{\mathrm{sw}} = f_{\mathrm{sw}} \cdot \frac{V_{\mathrm{dc}}}{V_{100\mathrm{FIT}}} \cdot \left(\frac{a}{2} + \frac{b \cdot I_{\max}}{\pi} + \frac{c \cdot I_{\max}^2}{4} \right) \tag{6}$$

Thermal model

The equivalent average thermal circuit is used to calculate the maximum allowable thermal resistance to keep junction temperature in the semiconductors under the safe thresholds. However, as one of the objectives of this paper is to evaluate the volume of the converter, a calculation to relate the maximum allowable thermal resistance with the required CS volume needs to be added. To do so, commercial CSs with forced air are analyzed. The required volume and the achieved thermal resistance are plotted for each product, in order to identify a trend that can be approximated with an exponential curve, shown with a black line, Fig. 5 (a). Every technology has different power losses, and as the switching frequency also affects the power losses, every semiconductor and selected switching frequency combination will require a maximum thermal resistance. Using the exponential approximation of the available commercial CSs, the thermal model is capable to calculate the volume required in the cooling system for every semiconductor technology and switching frequency combination.

Filter model

A line filter is added in the output of the back-to-back converter to shape the output current, as shown in Fig. 1. The inductance and capacitance values in the filter are calculated using expressions (7) and (8) presented in [23].and [24] respectively. V_{dc} is 1200V , ΔI_{out} is defined as 10 % of the I_{out} and Att_{req}, which refers to the required attenuation of the filter, is set to 0.01 in order to have enough damping in the switching frequency [25]. m refers to the converter topology level, 2 in this case, as a 2L-VSC converter is used.

$$L_f = \frac{V_{dc}}{6(m-1) \cdot \Delta I_{out} \cdot f_{sw}} \tag{7}$$

$$C_f = \frac{1}{(2\pi \cdot f_{sw})^2 \cdot L_f \cdot Att_{req}} \tag{8}$$

To calculate the volume of the inductor, the area product A_p technique proposed in [26] is used. Equation (9) uses the factor k_L to relate the area product and inductor volume. As this factor is dependent on the switching frequency, a polynomial approximation is performed to calculate k_L in [27], and shown in (10). In the case of the capacitor, [24] identifies a relation between volume, the rated voltage and capacitance for every technology. To estimate the required volume, commercial foil capacitors are analyzed, considering their volume and rated voltage, Fig. 5(b). It is identified that the volume is linearly dependent on the rated capacitance, for a same rated voltage. 1.2 kV series is selected, and the linear expression shown in (11), represented with a black line in Fig. 5(b), is used to estimate the required capacitors volume in the filter, introducing the capacitance value C_f in micro farads (μF).

$$Vol_{L_f} = k_L \cdot A_p{}^{\frac{3}{4}} \tag{9}$$

$$k_L = 2.676 \times 10^{-5} \cdot f_{sw} + 19.71 \tag{10}$$

$$Vol_{C_f} = 0.004 C_f + 0.0084 \tag{11}$$

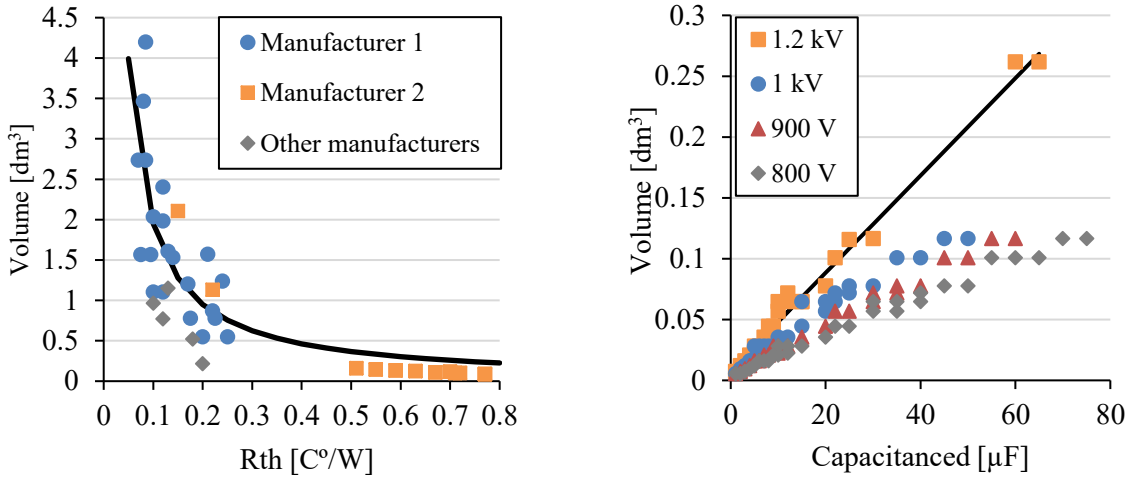

(a) (b)

Fig. 5: Volumes of different commercial components, (a) cooling systems, (b) capacitors.

Simulation and discussion

In this section, the performed study is presented. Three main analysis are done: the CSs volume and converters efficiency optimization, the filter volume optimization without penalizing efficiency and total volume optimization. The cooling system and the magnetic components are the major contributors to the volume of a power converter [28], [29], being the power semiconductors volume negligible. In the case of the analyzed back-to-back converters, the volume of the converters is mainly the one of the cooling system, however, the volume of the filter is considered as part of the converter, playing an important role in the total volume of the system. dc bus capacitors volume, control boards and the volume required for connections is not considered in this analysis.

Fixed switching frequency for CS volume and converter efficiency optimization

First, the state-of-the-art WGS nominal operation is tested for the three semiconductor technologies. Switching frequency is set to 2.5 kHz, and the systems efficiency is tested in all the wind speed range, from 3 to 25 m/s, with the three semiconductor technologies, Fig. 6. The efficiency with SiC MOSFETs is higher in all wind speed range, being the efficiency with Si IGBTs the lowest. Maximum power is extracted from the wind turbine from nominal wind speed (12.5 m/s) to maximum wind speed (25 m/s), however, due to the rotor angular speed, the converter manages maximum power at maximum wind speed, Fig. 3, being this the point in where maximum losses occur. The maximum losses in the power converter are considered to calculate the required cooling system volume for each semiconductor technology, Table II.

Table II shows that an 11.92 kW loss reduction is achieved by replacing Si IGBTs with SiC MOSFETs. This reduction means a 2.02 % increment in the converter efficiency at the maximum loss point, and can bring a 53.01 % reduction in the cooling system volume. If hybrid devices are used, the achieved CS volume reduction is 33.83 %.

Table II: Evaluation of the converter losses and required CS volume at 25 m/s wind speed

Technology	Maximum power losses [kW]	Efficiency [%]	Required CSs volume [dm³]	Required CS volume reduction [%]
Si IGBT	20.16	95.62	25.32	/
Hybrid	13.25	96.72	16.75	33.83
SiC MOSFET	8.24	97.64	11.89	53.01

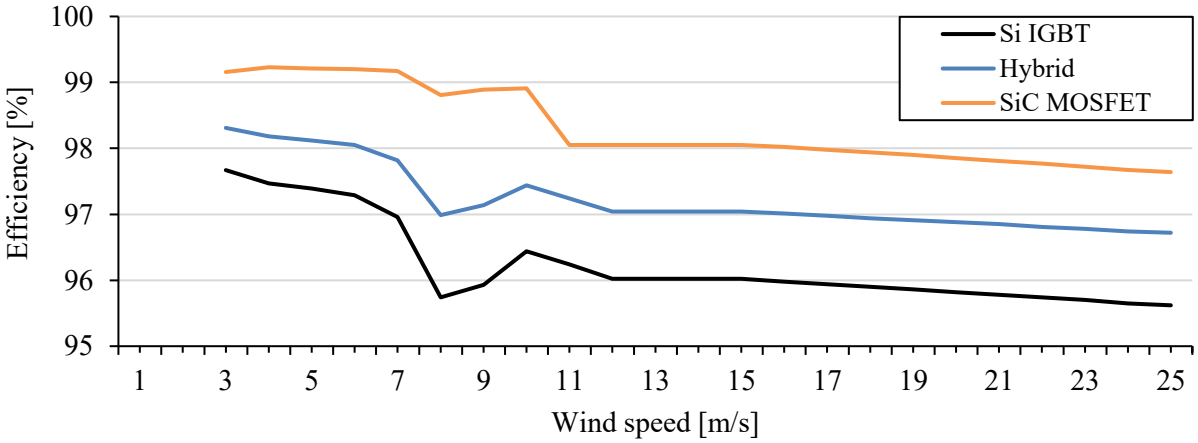

Fig. 6: Converter efficiency for different semiconductor technologies and wind speeds.

Switching frequency increment and filter volume evaluation

A second analysis is done varying the switching frequency of the converter. According to the device analysis done previously and shown in Fig. 4 (b), the energy required to switch SiC MOSFETs and Hybrid devices is lower than the one required in Si IGBTs. This characteristic allows to increase the switching frequency using SiC based devices, without penalizing efficiency. As the converter spends most of the time working at nominal wind speed (12.5 m/s), the evolution of power losses varying switching frequency at this wind speed is analyzed, Fig. 7. Even if the three technologies efficiency decreases linearly with switching frequency, the slope in SiC based converters is smaller than in the Si IGBTs. Hybrid devices switching frequency can be increased up to 4 kHz, while SiC MOSFETs can increase their frequency up to 23 kHz until Si IGBTs losses are matched.

Using equations (7)-(11) the volume required for the line filter in a range of switching frequencies is computed and plotted, Fig. 8, concluding that the filter volume is reduced exponentially with increasing frequency. Rising the switching frequency from 2.5 kHz to 4 kHz a filter reduction of 29.38 % is achieved using hybrid devices, while increasing the switching frequency up to 23 kHz with SiC MOSFETs can reduce the filter volume in 80.09 %, achieving filter volumes smaller than 1 dm^3, without penalizing converters efficiency, Table III.

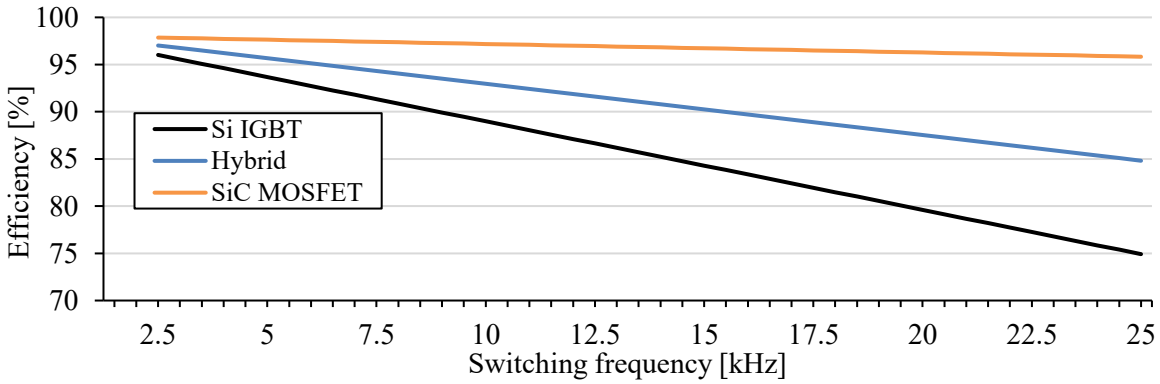

Fig. 7: Converter efficiency for different semiconductor technology and switching frequencies, at nominal wind speed.

Table III: Required filter volume reduction

Technology	Switching frequency [kHz]	Required filter volume [dm^3]	Required filter volume reduction [%]
Si IGBT	2.5	4.42	/
Hybrid	4	3.12	29.38
SiC MOSFET	23	0.88	80.09

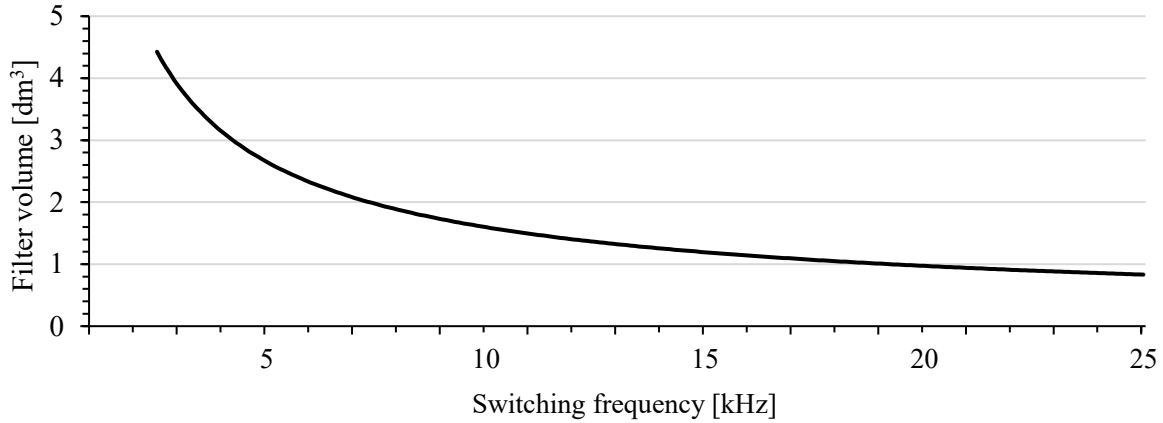

Fig. 8: Volume of the required filter for different switching frequencies.

Volume optimization and optimum switching frequency evaluation

In this final approach, the total volume of the converter is optimized. Table II shows the volume reduction achieved with SiC devices in the CS. In addition, the volume reduction in the filter due to increased switched frequency is seen in Fig. 8. A combination of both volume reductions is pursued in this section, but as Fig. 7 shows, increasing switching frequency to obtain a volume reduction in the filter also increases the converter losses, increasing the required CS volume to keep the semiconductors junction temperature under an adequate threshold (150 ºC). Fig. 9 shows the required CSs volume for every semiconductor technology and different switching frequencies. As only SiC MOSFETs keep cooling systems volume under reasonable limits compared to the filter volume, Fig. 8 and Fig. 9, the converters volume optimization is only performed for SiC MOSFETs. In converters with Si IGBTs and Hybrid devices, the total volume will be dominated by the CS; not getting any volume reduction when increasing the switching frequency.

The filter volume, Fig. 8, and the required volume for the cooling system for SiC MOSFETs, represented by the orange line in Fig. 9, are added in order to evaluate the optimum switching frequency to obtain minimum volume. This analysis is shown in Fig. 10, where filter volume, CS volume and combined volume can be seen for a SiC MOSFET based converter at different switching frequencies. The minimum combined volume is achieved at 4.5 kHz switching frequency, being 15.69 dm^3. As it has been seen in Fig. 7, the SiC MOSFET converter has still better efficiency than the Si IGBT converter at 4.5 kHz switching frequency and nominal wind speed, so with this optimized design, CS volume, filter volume and efficiency at nominal wind speed are improved with respect to Si IGBT based converter, Table IV. It must be considered that dc link capacitor, as well as the volume of semiconductors, connections and control boards is not considered in this analysis.

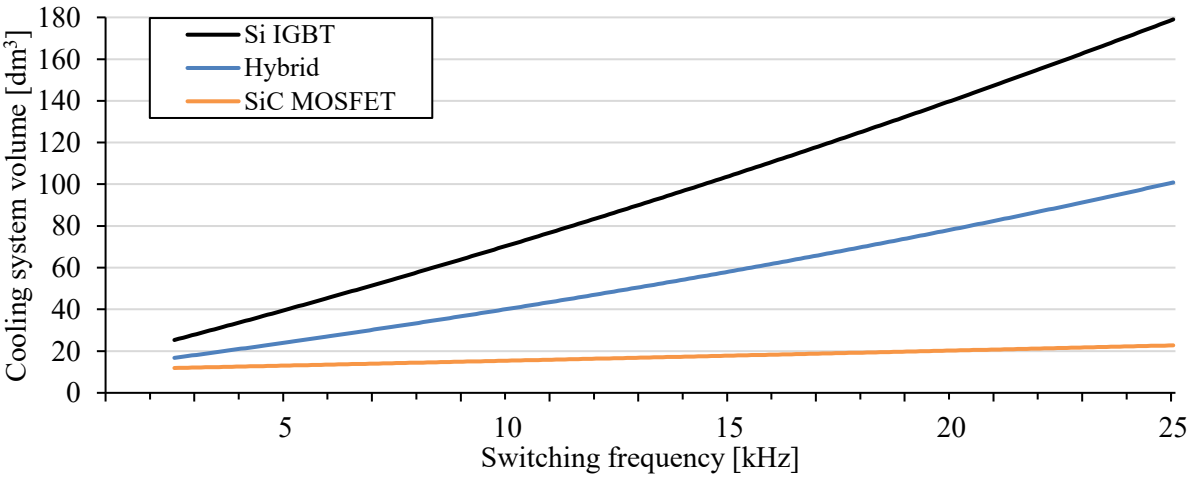

Fig. 9: Required cooling systems volume for different semiconductor technologies and switching frequencies.

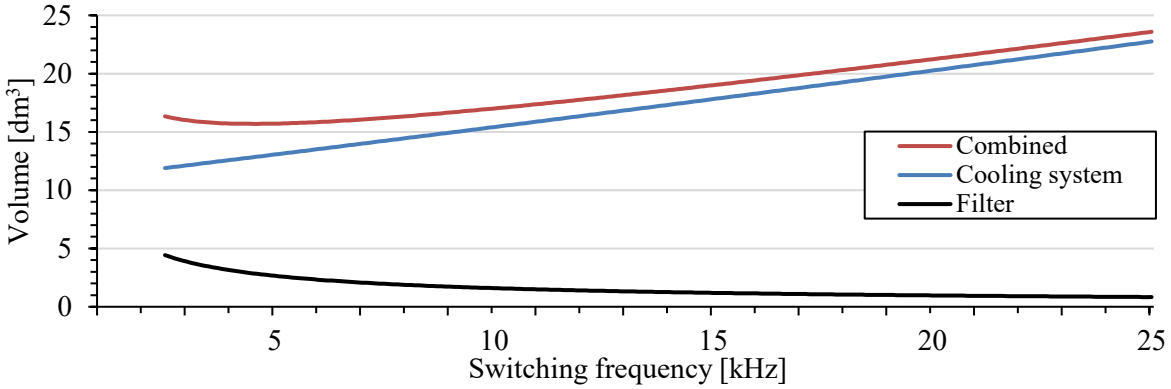

Fig. 10: Filter, cooling system and combined volume for SiC MOSFET based converter for different switching frequencies.

Table IV: Optimized SiC MOSFET based converter characteristics, compared to Si IGBT based converter

Characteristic	Si IGBT	Optimized SiC MOSFET	Unit
Switching frequency	2.5	4.5	kHz
Efficiency at nominal wind speed	96.02	97.67	%
Filter volume	4.42	2.86	dm^3
Filter volume reduction	/	35.29	%
Required CS volume	25.88	12.83	dm^3
Required CS volume reduction	/	50.42	%
Combined volume	30.30	15.69	dm^3
Combined volume reduction	/	48.21	%

Conclusion

This work has lead to the conclusion that SiC semiconductors can have an impact in DFIG based WESs power converter design, taking advantage of their superior conduction and mostly switching characteristics. Si IGBTs one to one replacement with hybrid devices or SiC MOSFETs can achieve efficiency improvement together with cooling systems requirements reduction, maintaining the same switching frequency. If switching frequency is increased in SiC devices, until the power losses are equaled to those of IGBTs, the output filters volume can significantly be reduced. This paper also identifies an optimum switching frequency to obtain minimum converter volume for a SiC MOSFET based converter. If this strategy is adopted, cooling system and output filter volumes are reduced with respect to the Si IGBT converter, and the efficiency at nominal wind speed operation point is still improved.

For these reasons, it is concluded that SiC semiconductors impact in DFIG based WES is favorable not only from the efficiency point of view, but also contributing to reduce auxiliary systems requirements like the cooling system and output filter, achieving a 48.21 % of the combined volume reduction. The inclusion of the volume required for the dc link capacitor, control boards, power semiconductors and connections should be analyzed in the future, as it is not considered in this analysis. In addition, any cost consideration will require the contribution of SiC semiconductors manufacturers, to evaluate the impact on the overall cost of the system.

References

[1] "2019 Was the Second-Hottest Year Ever, Closing Out the Warmest Decade - The New York Times." [Online]. Available: https://www.nytimes.com/interactive/2020/01/15/climate/hottest-year-2019.html. [Accessed: 17-Jan-2020].

[2] "Transforming our world: the 2030 Agenda for Sustainable Development .:. Sustainable Development Knowledge Platform." [Online]. Available: https://sustainabledevelopment.un.org/post2015/transformingourworld. [Accessed: 09-Jan-2020].

[3] "Mission area: Adaptation to climate change including societal transformation | European Commission." [Online]. Available: https://ec.europa.eu/info/horizon-europe-next-research-and-innovation-framework-programme/mission-area-adaptation-climate-change-including-societal-transformation_en. [Accessed: 09-Jan-2020].

[4] Kusch-Brandt, *Urban Renewable Energy on the Upswing: A Spotlight on Renewable Energy in Cities in REN21's "Renewables 2019 Global Status Report,"* vol. 8, no. 3. 2019.

[5] I. Dincer, "Renewable energy and sustainable development: A crucial review," *Renew. Sustain. energy Rev.*, vol. 4, no. 2, pp. 157–175, Jun. 2000.

[6] S. R. Bull, "Renewable energy today and tomorrow," *Proc. IEEE*, vol. 89, no. 8, pp. 1216–1226, 2001.

[7] J. He, T. Zhao, X. Jing, and N. A. O. Demerdash, "Application of wide bandgap devices in renewable energy systems - Benefits and challenges," in *3rd International Conference on Renewable Energy Research and Applications, ICRERA 2014*, 2014, pp. 749–754.

[8] M. Furuhashi, S. Tomohisa, T. Kuroiwa, and S. Yamakawa, "Practical applications of SiC-MOSFETs and further developments," *Semicond. Sci. Technol.*, vol. 31, no. 3, Jan. 2016.

[9] H. Zhang and L. M. Tolbert, "Efficiency Impact of Silicon Carbide Power Electronics for Modern Wind Turbine Full Scale Frequency Converter," *IEEE Trans. Ind. Electron.*, vol. 58, no. 1, 2011.

[10] C. Sintamarean, E. Eni, F. Blaabjerg, R. Teodorescu, and H. Wang, "Wide-band gap devices in PV systems - Opportunities and challenges," in *2014 International Power Electronics Conference, IPEC-Hiroshima - ECCE Asia 2014*, 2014, pp. 1912–1919.

[11] R. C. Portillo *et al.*, "Modeling strategy for back-to-back three-level converters applied to high-power wind turbines," *IEEE Trans. Ind. Electron.*, vol. 53, no. 5, pp. 1483–1491, Oct. 2006.

[12] M. Van Dessel and G. Deconinck, "Power electronic grid connection of PM synchronous generator for wind turbines," in *IECON Proceedings (Industrial Electronics Conference)*, 2008, pp. 2200–2205.

[13] A. Castellazzi, E. Gurpinar, Z. Wang, A. S. Hussein, and P. G. Fernandez, "Impact of wide-bandgap technology on renewable energy and smart-grid power conversion applications including storage," *Energies*, vol. 12, no. 23, pp. 1–14, 2019.

[14] A. Hussein and A. Castellazzi, "Comprehensive design optimization of a wind power converter using SiC technology," in *6th IEEE International Conference on Smart Grid, icSmartGrids 2018*, 2019, pp. 34–38.

[15] E. Of, "SiC-Based Power Electronics for Wind Energy Applications Acknowledgments," 2018.

[16] H. Zhang and L. M. Tolbert, "SiC's Potential Impact on the Design of Wind Generation System," 2008.

[17] R. Dey and S. Nath, "Replacing silicon IGBTs with SiC IGBTs in medium voltage wind energy conversion systems," in *India International Conference on Power Electronics, IICPE*, 2017, vol. 2016-Novem.

[18] W. L. Erdman, J. Keller, D. Grider, and E. Vanbrunt, "A 2.3-MW Medium-voltage, three-level wind energy inverter applying a unique bus structure and 4.5-kV Si/SiC hybrid isolated power modules," in *Conference Proceedings - IEEE Applied Power Electronics Conference and Exposition - APEC*, 2015, vol. 2015-May, no. May, pp. 1282–1289.

[19] I. Kortazar, I. Larrazabal, and P. Friedrichs, "Analysis of hybrid modules with Silicon Carbide diodes, comparison with full silicon devices and the impact in Wind applications," in *2016 18th European Conference on Power Electronics and Applications, EPE 2016 ECCE Europe*, 2016.

[20] A. Hussein and A. Castellazzi, "Variable frequency control and filter design for optimum energy extraction from a SiC wind inverter," in *2018 International Power Electronics Conference, IPEC-Niigata - ECCE Asia 2018*, 2018, pp. 2932–2937.

[21] G. Abad, J. López, M. A. Rodríguez, L. Marroyo, and G. Iwanski, *Doubly Fed Induction Machine*. 2011.

[22] B. Ozpineci, L. M. Tolbert, S. K. Islam, and M. Hasanuzzaman, "Effects of silicon carbide (SiC) power devices on HEV PWM inverter losses," *IECON Proc. (Industrial Electron. Conf.*, vol. 2, no. C, pp. 1061–1066, 2001.

[23] M. Mazuela, "Análisis y desarrollo de una novedosa topología de convertidor multinivel para aplicaciones de media tensión y alta potencia," Mondragon Unibertsitatea, 2015.

[24] J. W. Kolar *et al.*, "PWM converter power density barriers," *Fourth Power Convers. Conf. PCC-NAGOYA 2007 - Conf. Proc.*, no. May, 2007.

[25] A. Anthon, Z. Zhang, M. A. E. Andersen, D. G. Holmes, B. McGrath, and C. A. Teixeira, "The benefits of SiC mosfets in a T-type inverter for grid-tie applications," *IEEE Trans. Power Electron.*, vol. 32, no. 4, pp. 2808–2821, 2017.

[26] W. G. Hurley and W. H. Wölfle, *Transformers and inductors for power electronics: theory, design and applications*. Wiley-Blackwell, 2013.

[27] E. Gurpinar and A. Castellazzi, "Single-Phase T-Type Inverter Performance Benchmark Using Si IGBTs, SiC MOSFETs, and GaN HEMTs," *IEEE Trans. Power Electron.*, vol. 31, no. 10, pp. 7148–7160, Oct. 2016.

[28] G. Ortiz, M. Leibl, J. W. Kolar, and O. Apeldoorn, "Medium frequency transformers for solid-state-transformer applications - Design and experimental verification," *Proc. Int. Conf. Power Electron. Drive Syst.*, pp. 1285–1290, 2013.

[29] U. Drofenik and J. W. Kolar, "Analyzing the Theoretical Limits of Forced Air-Cooling by Employing Advanced Composite Materials with Thermal Conductivities," 2011.